AIP | Applied Physics Letters

Magnetocrystalline anisotropy behavior in the multiferroic BiMnO3 examined by Lorentz transmission electron microscopy

T. Asaka, M. Nagao, T. Yokosawa, K. Kokui, E. Takayama-Muromachi, K. Kimoto, K. Fukuda, and Y. Matsui

Citation: Applied Physics Letters **101**, 052407 (2012); doi: 10.1063/1.4742747
View online: http://dx.doi.org/10.1063/1.4742747
View Table of Contents: http://scitation.aip.org/content/aip/journal/apl/101/5?ver=pdfcov
Published by the AIP Publishing

Magnetocrystalline anisotropy behavior in the multiferroic $BiMnO_3$ examined by Lorentz transmission electron microscopy

T. Asaka,[1] M. Nagao,[2] T. Yokosawa,[2] K. Kokui,[1] E. Takayama-Muromachi,[2] K. Kimoto,[2] K. Fukuda,[1] and Y. Matsui[2]
[1]*Department of Materials Science and Engineering, Nagoya Institute of Technology, Nagoya 466-8555, Japan*
[2]*National Institute for Materials Science, Tsukuba 305-0044, Japan*

(Received 3 April 2012; accepted 23 July 2012; published online 3 August 2012)

We investigated magnetic domain structures of a multiferroic manganite, $BiMnO_3$, by Lorentz transmission electron microscopy. Ferromagnetic domains were observed below ~105 K, close to the ferromagnetic Curie temperature, T_C. The spontaneous magnetization aligns distinctly along the [010] direction, suggesting that the magnetic easy direction is along the *b* axis. Inflection and merging of the domain walls was observed at twin boundaries. This indicates pinning of the magnetic domain walls at crystallographic twin boundaries. Furthermore, we observed narrow magnetic domain walls, suggesting strong magnetocrystalline anisotropy. © *2012 American Institute of Physics*. [http://dx.doi.org/10.1063/1.4742747]

$BiMnO_3$ has recently attracted a lot of attention as a "multiferroic" material in which ferroelectricity and ferromagnetism coexist.[1,2] Multiferroic materials are of interest with respect to the coupling between the ferroelectricity and the ferromagnetism and their possible control by the application of magnetic and/or electric fields.[3–7] $BiMnO_3$ exhibits ferromagnetism below $T_C \sim 100$ K and a saturation magnetization of ~3.6 μB.[8,9] Furthermore, ferroelectricity has been observed below $T_{FE} \sim 450$ K by Moreira dos Santos *et al.*[1] The ferroelectric remanent polarization was reported to be 0.043 $\mu C/cm^2$ at 200 K. The ferroelectricity is attributed to the noncentrosymmetric crystal structure, monoclinic *C*2 ($a \approx 9.53$ Å, $b \approx 5.61$ Å, $c \approx 9.85$ Å, and $\beta \approx 110.67°$ at room temperature).[10,11] The *C*2 structure has been confirmed by neutron diffraction[10,11] and electron diffraction[10,12] studies. Meanwhile, $BiMnO_3$ has a complicated three-dimensional orbital ordering structure.[10,11,13] Here the spontaneous electric polarization occurs along the *b* axis in the monoclinic cell.

The ferromagnetic and ferroelectric structures in $BiMnO_3$ are considered to be led and stabilized by orbital-ordering[11] and crystal-lattice distortions derived from covalent bonding between Bi and O (Refs. 11 and 14) and Bi $6s^2$ lone pairs.[10,15] Concerning interactions between the ferromagnetism and the ferroelectricity, Kimura *et al.* have demonstrated the magnetodielectic effect around T_C.[16] Furthermore, other multiferroic properties, such as the change in the polar symmetry of optical second-harmonic generation signals under external magnetic fields[17] and the magnetoelastic strain involved with the magnetodielectric behavior[18] have been reported. It is important to obtain details of the interactions among the magnetic, electric, and crystallographic structures of multiferroics from a physics perspective as well as seeking realistic applications for magnetoelectric devices. In this work, we investigated relationships between magnetic domain and crystallographic structures in $BiMnO_3$ by means of transmission electron microscopy (TEM). The observed ferromagnetic and crystallographic structures suggested pinning of the magnetic domains at the twin boundaries and strong magnetocrystalline anisotropy.

The examined polycrystalline samples were obtained by high-pressure synthesis following Ref. 10. The samples were checked by x-ray powder diffraction to confirm sample quality. The sample consists of a majority phase of $BiMnO_3$ and a trace of $Bi_2O_2CO_3$. Magnetization measurements were performed using a commercial SQUID magnetometer. TEM enables us to obtain crystallographic and magnetic information concurrently in both reciprocal and real spaces.[19] For observations using TEM, the samples were thinned by mechanical grinding and Ar^+ ion sputtering. We employed selected area electron diffraction (SAED), bright- and dark-field imaging, and Lorentz transmission electron microscopy (LTEM) imaging, using a dedicated Lorentz electron microscope (Hitachi, HF-3000L) operating at 300 kV with a low-temperature system. The TEM specimens were cooled from room temperature to 19 K in a liquid-helium cooling holder. We used the conventional Fresnel method for the magnetic domain imaging[20] and analyzed the Fresnel images using the commercial software QPt for DigitalMicrograph,[21] which enabled us to quantitatively compute the phase changes of electron waves and magnetic components of the local magnetization perpendicular to the electron propagation direction, based on the transport-of-intensity equation (TIE).[22,23]

Figure 1 shows the temperature dependence of magnetization and LTEM images below and above T_C. The present $BiMnO_3$ sample shows ferromagnetism below $T_C \sim 110$ K (Fig. 1(a)). In the LTEM observation, we could observe a ferromagnetic domain structure below ~105 K, close to T_C. Figure 1(b) displays a LTEM image at 95 K, taken with an over-focus of 0.5 mm. Both bright and dark lines correspond to magnetic domain walls. This image indicates that the present sample has a spontaneous magnetization at this temperature. Upon heating, the magnetic domain walls disappeared above 105 K, as seen from the LTEM image taken at 120 K in Fig. 1(c), because the system entered the paramagnetic state. Note that dark lines, indicated by arrows in Fig. 1(c), represent twin boundaries between the twin variants perpendicular to the [112] and $[\bar{1}1\bar{2}]$ directions. From Fig. 1(b) and inset, the sharp bright and broad dark lines that correspond to the

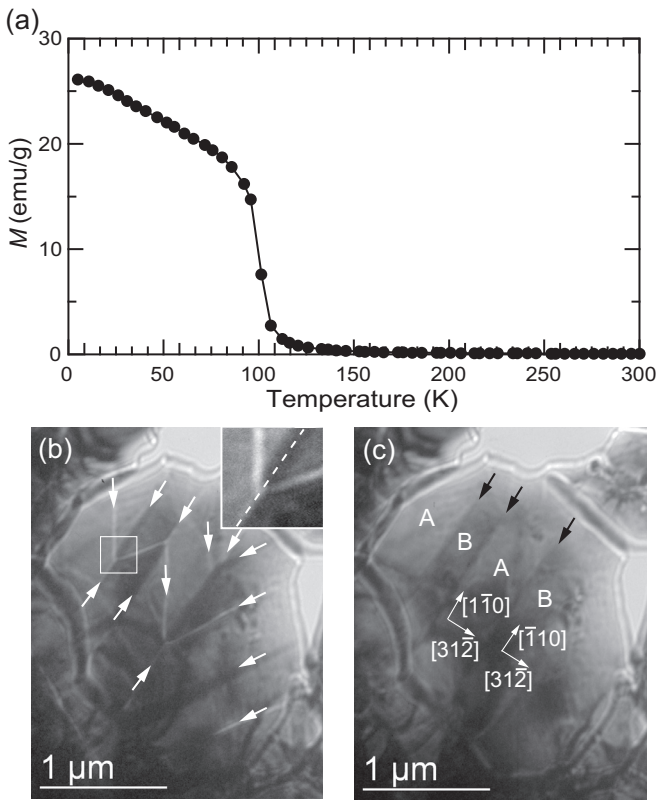

FIG. 1. (a) Temperature dependence of magnetization, applying magnetic fields of 1000 Oe after cooling under 1000 Oe. LTEM images at (b) 95 K ($T < T_C$) and (c) 120 K ($T > T_C$). White arrows in (b) represent magnetic domain walls. Black arrows in (c) represent twin boundaries. Labels "A" and "B" in (c) denote twin variants. The twin variants A and B are oriented perpendicular to the [112] and [$\bar{1}$1$\bar{2}$] directions, respectively. The inset of (b) is the magnified image corresponding to the framed region in (b). A dashed line indicates a twin boundary.

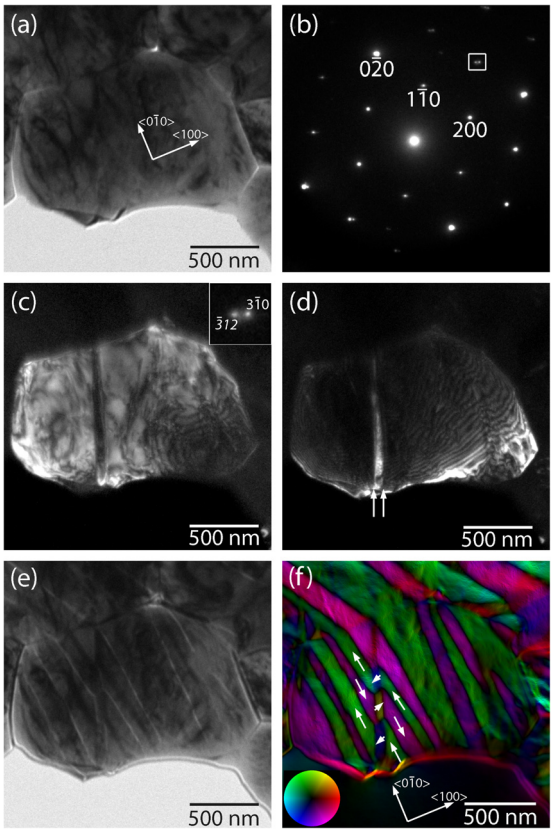

FIG. 2. Magnetic domain and crystallographic structures at 19 K. (a) A bright-field image and an electron diffraction pattern for a grain oriented perpendicular to [001] (majority) and [1$\bar{1}$2] (minority). Dark-field images formed with the (c) 3$\bar{1}$0 and (d) $\bar{3}$12 diffraction spots for the [001] and [1$\bar{1}$2] twin variants, respectively. The inset of (c) is the magnified image of the framed region in (b). White arrows in (c) indicate twin boundaries. (e) LTEM image taken with over-focus of 0.5 mm. (d) Magnetization-distribution map derived by the TIE method. White arrows represent approximate magnetization directions in the respective domains. The inset is a color wheel for the interpretation of the magnetization-distribution map.

magnetic domain walls were observed on the twin boundaries. This indicates that the twin boundaries play a role as pinning sites of the magnetic domains. This is analogous to pinning in other ferromagnetic manganites.[24,25] We note that the observed twin structure seems to be a ferroelastic-domain-like configuration in terms of the crystallographic texture, which is also related to the ferroelectric materials.

The LTEM observation revealed strong magnetocrystalline anisotropy in $BiMnO_3$. Figure 2 shows the relationship between the crystallographic and magnetic domain structures. The grain is oriented mainly perpendicular to [001] (Fig. 2(a)), as indicated by the corresponding electron diffraction pattern (Fig. 2(b)). Splitting of diffraction spots in the higher-order region could be recognized clearly, indicating presence of a twin variant oriented perpendicular to [1$\bar{1}$2]. We performed dark-field imaging using both of the diffraction spots inside the white frame in Fig. 2(b). Figures 2(c) and 2(d) show the respective dark-field images formed with the 3$\bar{1}$0 diffraction spot for the majority twin variant and the $\bar{3}$12 diffraction spot for the minority one. Bright regions in each image represent the corresponding twin variants. A narrow twin domain oriented perpendicular to [1$\bar{1}$2] lies between the majority [001] twin domains. Figure 2(e) shows a LTEM image at 19 K. Dark and bright lines representing magnetic domain walls were observed. The magnetic domain walls were found to develop along the [010] direction in the majority twin domains. Figure 2(f) shows the local magnetization-distribution map calculated using the TIE method. The inset of Fig. 2(f) is a color wheel for interpretation of the magnetization-distribution map, where the color and its intensity represent the respective direction and magnitude of the magnetic moment. The magnetic moments clearly orient along the [010] direction in the majority twin domains, forming a 180°-domain structure. This suggests that the magnetic easy direction is along the *b* axis in the monoclinic cell. This is consistent with the result of a previous neutron diffraction study.[11] Interestingly, although the [001] and [1$\bar{1}$2] directions are equivalent in the primitive cubic perovskite, the magnetic moments inflect at the twin boundaries and their components perpendicular to the electron propagation direction are along a projection of the [010] direction in the minority [1$\bar{1}$2] twin domain. This suggests that the easy direction of magnetization is properly confined to the *b* axis in the monoclinic cell.

We measured the width of magnetic domain walls in $BiMnO_3$. Figure 3(a) shows a LTEM image of the narrowest magnetic domain wall observed, which was taken with the incident electron beam nearly parallel to the magnetic domain wall, the so-called "edge-on condition." We calculated the electron-phase change from the LTEM images by the TIE

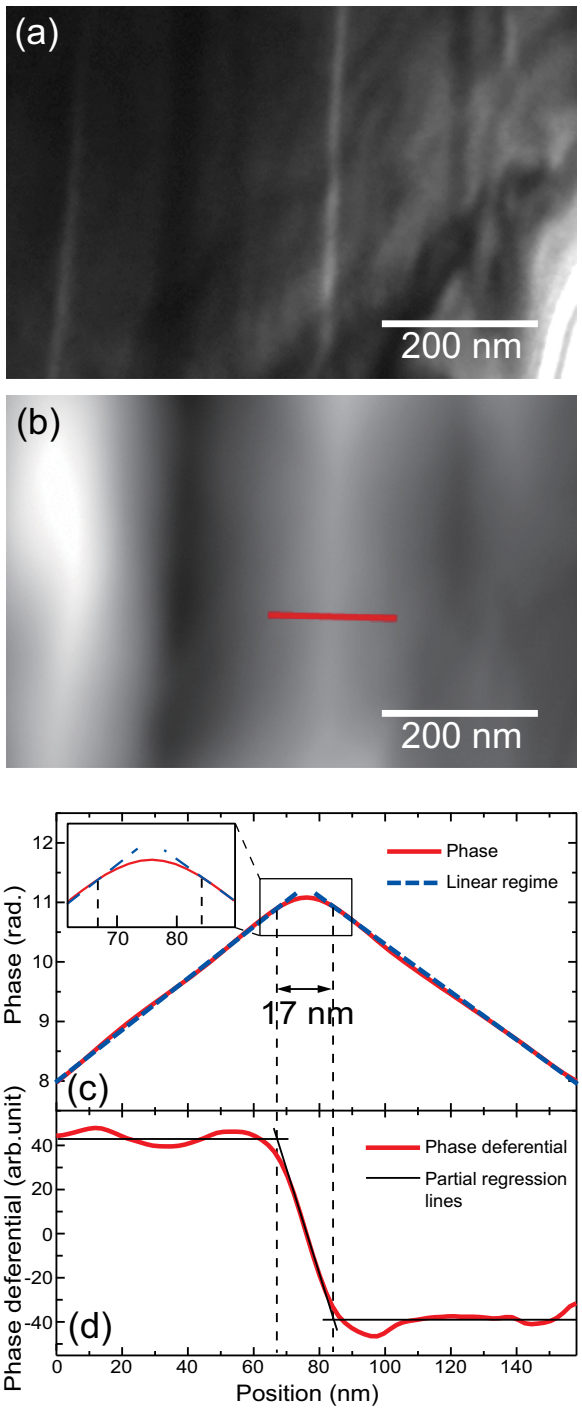

FIG. 3. (a) LTEM and (b) phase images of the magnetic domains. The phase image (b) was derived from the LTEM images with the TIE method. (c) A phase profile along the line in (b). Dashed lines represent linear regime of the phase profile. The inset is an expanded view of the boxed region. (d) A differential of the phase profile of (c). Flat parts and steep slope of the regression lines correspond to the magnetic domains and the domain walls, respectively.

method (Fig. 3(b)). Here, the main contribution of the phase change is from the magnetic fields in the phase image of the ferromagnetic sample. Figures 3(c) and 3(d), respectively, show a phase profile and its phase differential of the propagated electron wave along the line in Fig. 3(b). Parts of the linear profile in Fig. 3(c) correspond to the region inside the magnetic domains, whereas flat parts and steep slope of the regression lines in Fig. 3(d) correspond to the magnetic domains and the domain walls, respectively. Thus, in both Figs. 3(c) and 3(d), the magnetic domain wall measures ~17 nm in width. This measurement method is analogous with that using electron holography.[26] The width of the present magnetic domain wall is relatively narrow for those in the ferromagnetic manganites (typically more than 30 nm).[27,28] This suggests that $BiMnO_3$ has relatively strong magnetocrystalline anisotropy characterized by the magnetic easy direction of the *b* axis. We consider that the origin of magnetocrystalline anisotropy is likely due to the lower crystal symmetry and the complicated orbital ordering.

We could not observe evident ferroelectric domain walls, such as a 180°-ferroelectric domain wall along the *b* axis. This might be caused by a small electric polarization in this system, or $BiMnO_3$ has a centrosymmetric crystal structure, *C*2/*c*; that is, $BiMnO_3$ is not a ferroelectric material, as mentioned in previous reports.[29,30] We cannot determine from our observations whether $BiMnO_3$ is ferroelectric. However, we note that if the system exhibits ferroelectricity, twin boundaries may act as possible ferroelectric domain walls. Thus, taking into account the abovementioned pinning, the ferroelectric domain walls might couple with the magnetic domain walls in $BiMnO_3$. Furthermore, the coupling between the ferromagnetism, the ferroelectricity and the crystallographic elasticity might arise, since both the spontaneous magnetization and the electric polarization are along the crystallographic *b* axis.

In summary, we observed the magnetic domain structures that interact with the crystallographic structures in $BiMnO_3$. The observed domain structures and textures indicate pinning of the magnetic domains at the crystallographic twin boundaries and relatively strong magnetic anisotropy. These can give rise to strong coupling between the magnetic and crystallographic structures, as well as ferroelectricity.

We thank T. Nagai, X. Z. Yu, and W. Z. Zhang for their valuable discussions. Work by T.A. was supported by KAKENHI (No. 23740239) and a grant from Institute of Ceramics Research and Education, Nagoya Institute of Technology. A part of this work was supported by the Nanotechnology Network Project, MEXT, Japan.

[1]A. M. dos Santos, S. Parashar, A. R. Raju, Y. S. Zhao, A. K. Cheetham, and C. N. R. Rao, Solid State Commun. **122**, 49 (2002).
[2]Z. H. Chi, H. Yang, S. M. Feng, F. Y. Li, R. C. Yu, and C. Q. Jin, J. Magn. Magn. Mater. **310**, e358 (2006).
[3]H. Schmid, Ferroelectrics **162**, 317 (1994); H. Schmid, *ibid.* **221**, 9 (1999).
[4]J. Wang, J. B. Neaton, H. Zheng, V. Nagarajan, S. B. Ogale, B. Liu, D. Viehland, V. Vaithyanathan, D. G. Schlom, U. V. Waghmare, N. A. Spaldin, K. M. Rabe, M. Wuttig, and R. Ramesh, Science **299**, 1719 (2003).
[5]T. Kimura, T. Goto, H. Shintani, K. Ishizaka, T. Arima, and Y. Tokura, Nature (London) **426**, 55 (2003).
[6]N. Hur, S. Park, P. A. Sharma, J. S. Ahn, S. Guha, and S.-W. Cheong, Nature (London) **429**, 392 (2004).
[7]T. Kimura, G. Lawes, and A. P. Ramirez, Phys. Rev. Lett. **94**, 137201 (2005).
[8]F. Sugawara, S. Iida, Y. Syono, and S. Akimoto, J. Phys. Soc. Jpn. **20**, 1529 (1965); *ibid.* **25**, 1553 (1968).
[9]H. Chiba, T. Atou, and Y. Syono, J. Solid State Chem. **132**, 139 (1997).
[10]T. Atou, H. Chiba, K. Ohoyama, Y. Yamaguchi, and Y. Syono, J. Solid State Chem. **145**, 639 (1999).
[11]A. M. dos Santos, A. K. Cheetham, T. Atou, Y. Syono, Y. Yamaguchi, K. Ohoyama, H. Chiba, and C. N. R. Rao, Phys. Rev. B **66**, 064425 (2002).

[12]T. Yokosawa, A. A. Belik, T. Asaka, K. Kimoto, E. Takayama-Muromachi, and Y. Matsui, Phys. Rev. B **77**, 024111 (2008).
[13]C.-H. Yang, J. Koo, C. Song, T. Y. Koo, K.-B. Lee, and Y. H. Jeong, Phys. Rev. B **73**, 224112 (2006).
[14]N. A. Hill and K. M. Rabe, Phys. Rev. B **59**, 8759 (1999).
[15]R. Seshadri and N. A. Hill, Chem. Mater. **13**, 2892 (2001).
[16]T. Kimura, S. Kawamoto, I. Yamada, M. Azuma, M. Takano, and Y. Tokura, Phys. Rev. B **67**, 180401(R) (2003).
[17]A. Sharan, J. Lettieri, Y. Jia, W. Tian, X. Pan, D. G. Schlom, and V. Gopalan, Phys. Rev. B **69**, 214109 (2004).
[18]E. Montanari, G. Calestani, L. Righi, E. Gilioli, F. Bolzoni, K. S. Knight, and P. G. Radaelli, Phys. Rev. B **75**, 220101 (2007).
[19]T. Asaka, X. Z. Yu, Y. Tomioka, Y. Kaneko, T. Nagai, K. Kimoto, K. Ishizuka, Y. Tokura, and Y. Matsui, Phys. Rev. B **75**, 184440 (2007).
[20]P. J. Grundy and R. S. Tebble, Adv. Phys. **17**, 153 (1968).
[21]K. Ishizuka and B. Allman, J. Electron Microsc. **54**, 191 (2005).
[22]M. R. Teaque, J. Opt. Soc. Am. **73**, 1434 (1983).
[23]K. A. Nugent, T. E. Gureyev, D. F. Cookson, D. Paganin, and Z. Barnea, Phys. Rev. Lett. **77**, 2961 (1996).
[24]T. Asaka, Y. Anan, T. Nagai, S. Tsutsumi, H. Kuwahara, K. Kimoto, Y. Tokura, and Y. Matsui, Phys. Rev. Lett. **89**, 207203 (2002).
[25]X. Z. Yu, R.-W. Li, T. Asaka, K. Ishizuka, K. Kimoto, and Y. Matsui, Appl. Phys. Lett. **95**, 092504 (2009).
[26]M. R. McCartney and Y. Zhu, Appl. Phys. Lett. **72**, 1380 (1998).
[27]S. J. Lloyd, N. D. Mathur, J. C. Loudon, and P. A. Midgley, Phys. Rev. B **64**, 172407 (2001).
[28]T. Asaka and Y. Matsui (unpublished).
[29]A. A. Belik, S. Iikubo, T. Yokosawa, K. Kodama, N. Igawa, S. Shamoto, M. Azuma, M. Takano, K. Kimoto, Y. Matsui, and E. Takayama-Muromachi, J. Am. Chem. Soc. **129**, 971 (2007).
[30]P. Baettig, R. Seshadri, and N. A. Spaldin, J. Am. Chem. Soc. **129**, 9854 (2007).